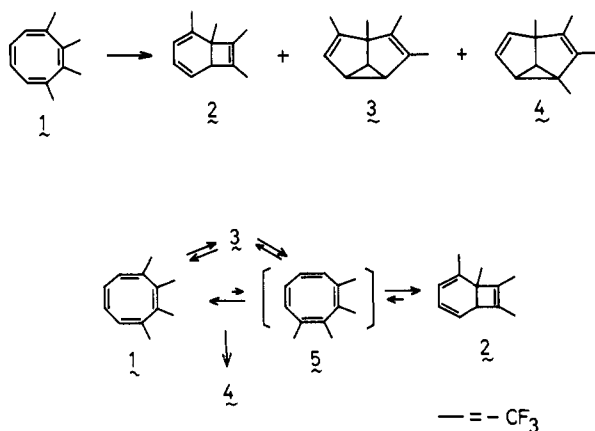Chart I

$$-\!=\!-\,CF_3$$

fluoromethyl)semibullvalenes. Compound **3** showed four multiplets at 6.44, 3.74, 3.42, and 3.30 ppm in ^{1}H NMR spectra. The last peak was assigned to be a methine proton at C-8 by the decoupling experiments. Chemical shifts and coupling pattern of these protons were quite similar to those of benzosemibullvalene.[9]

Next, we examined the variable-temperature ^{1}H NMR spectra from −90 to +120 °C, but any essential changes were not observed. Therefore, **3** was limited to one tautomer. Its ^{19}F and ^{13}C NMR spectra were consistent with this fixed structure. This might be due to the steric repulsion between the two trifluoromethyl groups on the 4 and 6 carbons, which inhibited its tautomerism. Compound **4** contrasted sharply with **3**. In the ^{1}H NMR spectra, one proton was in the olefinic region and another was in the methine region, while the other two were in the middle of these two regions. Therefore, **4** seemed to be in a very rapid Cope degeneration. However, its variable-temperature ^{1}H NMR spectra did not show any significant changes in the chemical shift and coupling pattern from −90 to 120 °C;[10] namely, **4** seemed to be a frozen-out intermediate of the Cope degeneration. Its ^{19}F and ^{13}C NMR spectra were consistent with this degenerate structure. This result shows a very interesting effect of trifluoromethyl groups. This might be due to the interaction between two allyl systems, one of which is substituted with three electronegative trifluoromethyl groups and the other is not.

Thermolysis of **3** at 170–180 °C gave a mixture of **1**, **2**, and **4**, which were ultimately converted to **4** on a prolonged heating, while the ratio of **1** and **2** was constant throughout the reaction. These results might be explained reasonably by the equilibrium shown in Chart I. Thus, **1** was in a thermal equilibrium with the bond-shift isomer **5**, which cyclized rapidly to **2**. Compound **1** and/or **5** were in a equilibrium with **3** and isomerized to the most stable isomer **4** among these compounds. The comparison of molecular models suggests that repulsion between the trifluoromethyl groups on 4 and 6 positions in **3** may explain the

(8) 3,4,5,6-Tetrakis(trifluoromethyl)tricyclo[3.3.0.0^{2,8}]octa-3,6-diene (**3**): colorless oil; IR (CCl$_4$) 1635, 1620 cm^{-1}; ^{1}H NMR (CDCl$_3$) δ 6.44 (7-H, br s), 3.74 (2-H, dd, $J_{1,2} = J_{2,8} = 6$ Hz), 3.42 (1-H, dd, $J_{1,2} = J_{1,8} = 6$ Hz), 3.3 (8-H, m); ^{19}F NMR (CDCl$_3$) δ (upward from C$_6$H$_5$CF$_3$) −7.92 (4-CF$_3$, m), −3.92 (6-CF$_3$, sept), −1.52 (3-CF$_3$, q), 5.6 (5-CF$_3$; qq); ^{13}C NMR (CDCl$_3$) δ 137.4, 136.3, 135.8 (d), 134.5, 122.6 (q), 120.7 (q), 119.8 (q), 70.6 (t), 55.1 (d), 40.2 (d), 39.5 (d); *m/e* 376 (M$^+$). 2,3,4,5-Tetrakis(trifluoromethyl)-tricyclo[3.3.0.0^{2,8}]octa-3,6-diene (**4**): colorless oil; IR (CCl$_4$) 1640, 1620 cm^{-1}; ^{1}H NMR (CDCl$_3$) δ 5.85 (7-H, dd, $J_{6,7} = J_{7,8} = 4$ Hz), 5.33 (6-H, d, $J_{6,7} = 4$ Hz), 4.75 (8-H, dd, $J_{1,8} = J_{7,8} = 4$ Hz), 3.78 (1-H, d, $J_{1,8} = 4$ Hz); ^{19}F NMR (CDCl$_3$) δ −4.8 (4-CF$_3$, sept), −3.2 (3-CF$_3$, sept), −2.6 (2-CF$_3$, q), 4.2 (5-CF$_3$, q); ^{13}C NMR (CDCl$_3$) δ 127.0 (d), 122.7 (q), 121.9 (q), 120.7 (q), 119.3 (q), 104.3 (q), 98.5 (d), 88.4 (q), 83.4 (d), 66.0 (q), 52.9 (d); *m/e* 376 (M$^+$).

(9) H. E. Zimmerman, R. S. Givens, and R. M. Pagni, *J. Am. Chem. Soc.*, **90**, 4191 (1968).

(10) At the temperature below −90 °C, compounds **3** and **4** crystallized from the solution. We could not observe their NMR spectra below this temperature.

higher stability of **4**. However, this should not be the only reason for this stability, since prolonged thermolysis of **4** did not give the cyclooctatetraene **1** at all. Therefore, this stability might be gained partially by the degenerate structure.
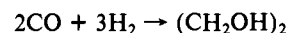
Ethylene Glycol from Synthesis Gas via Ruthenium Melt Catalysis

John F. Knifton

Texaco Chemical Company
Austin, Texas 78761

The preparation of ethylene glycol directly from synthesis gas (eq 1) via homogeneous rhodium,[1] ruthenium,[2] and cobalt[3] ca-

$$2CO + 3H_2 \rightarrow (CH_2OH)_2$$

$$\Delta G_{500} = +15.8 \text{ kcal/mol, } \log K_p = -6.9 \qquad (1)$$

talysis has generally been limited by the high pressures necessary to effect reaction[4] and the modest turnover frequencies.[1,5] The problem of high pressure can be partially overcome through the intermediate formation of vicinal glycol esters,[6–8] such as ethylene glycol diacetate (eq 2), where thermodynamic parameters are more

$$2CO + 3H_2 + 2HOAc \rightarrow (CH_2OAc)_2 + 2H_2O$$
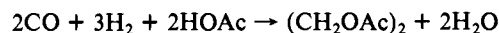
$$\Delta G_{500} = +4.7 \text{ kcal/mol, } \log K_p = -2.0 \qquad (2)$$

favorable.[8] In this paper we disclose a unique, highly active catalyst system for the direct synthesis of ethylene glycol (eq 1) involving ruthenium "melt" catalysis,[9] where the ruthenium source, such as ruthenium(IV) oxide or ruthenium(III) acetylacetonate, is dispersed in a molten quaternary phosphonium or ammonium salt such as tetrabutylphosphonium bromide.

While it is preferable that the ruthenium source and quaternary group 5B salt be solids at ambient temperatures, the melting point of the salt must lie well below the temperature necessary to effect CO hydrogenation[9] (ca. 220 °C). Under typical reaction temperature/pressure conditions then, the quaternary salt provides a highly polar, fluid medium for solubilization of the ruthenium active catalyst (vide infra) and effecting the desired conversion of synthesis gas to ethylene glycol. Alkanols plus diol are the major products. Data in Table I illustrate the preparation of ethylene glycol, together with glycol monoalkyl ethers and C$_1$–C$_2$ alkanols from CO/H$_2$ for a variety of ruthenium catalyst precursors and quaternary Group 5B salts.

The important features of this catalysis are the following: (a) The productivity of the melt catalysts—liquid weight gains[10] routinely exceed 100 wt% (see Table I, column 10) and turnover frequencies may surpass 7.8×10^{-3} s^{-1} at 220 °C (expt 16). (b) Glycol/alkanol weight ratios up to 1/1.65 have been noted, where ethylene glycol plus its monoalkyl ethers constitute >30 wt% of the liquid organic product. (c) Both alkanol and diol products may be readily isolated, by fractional distillation of the crude liquid

(1) Pruett, R. L. *Ann. N.Y. Acad. Sci.* **1977**, *295*, 239.
(2) Williamson, R. C.; Kobylinski, T. P. U.S. Patent 4 170 605, 1979.
(3) Gresham, W. F. U.S. Patent 2 636 046, 1953.
(4) Deluzarche, A.; Fonseca, R.; Jenner, G.; Kiennemann, A.; *Erdoel Kohle, Erdgas, Petrochem.* **1979**, *32*, 313.
(5) Walker, W. E.; Cropley, J. B. U.S. Patent 3 940 432, 1976. Kaplan, L. U.S. Patent 3 944 588, 1976.
(6) Knifton, J. F. British Patent 2 024 811, 1980.
(7) Dombek, B. D. *J. Am. Chem. Soc.* **1980**, *102*, 6855.
(8) Knifton, J. F. *J. Chem. Soc., Chem. Commun.* **1981**, 188.
(9) Knifton, J. F. U.S. Patent 4 265 828, 1981.
(10) Liquid weight gains, defined as (total liquid organic + aqueous products)/(total ruthenium catalyst + quaternary salt charged) × 100.

Table I. Glycol from Syngas–Ruthenium Melt Catalysis[a]

expt	ruthenium source	quaternary salt	mp, °C	added phosphine	product yield, mmol[b] $(CH_2\text{-}OH)_2$	$HOCH_2\text{-}CH_2OR$[c]	MeOH	EtOH	total liquid yield, wt %[d]
1	RuO_2	Bu_4PBr	100		56	64	242	120	166
2	$Ru(acac)_3$	Bu_4PBr	100		48	66	253	225	186
3	$Ru_3(CO)_{12}$	Bu_4PBr	100		25	45	251	181	160
4	$[Bu_4P][HRu_3(CO)_{11}]$	Bu_4PBr	100		39	37	237	183	162
5	$[Bu_4P]_2[Ru_6(CO)_{18}]$	Bu_4PBr	100		8	4	139	11	113
6	$RuO_2 \cdot xH_2O$	Bu_4PBr	100		34	53	250	204	193
7	$RuO_2 \cdot xH_2O$	Bu_4PCl	61		11	58	224	127	184
8	$RuO_2 \cdot xH_2O$	Bu_4PI	96		6	8	275	211	154
9	$RuO_2 \cdot xH_2O$	Bu_4POAc	73		10	14[e]	118[f]	9	59
10	$RuO_2 \cdot xH_2O$	Bu_4POH			8	9	206	36	83
11	$RuO_2 \cdot xH_2O$	$C_{16}H_{33}Bu_3PBr$	54		14	23	456	252	217
12	$RuO_2 \cdot xH_2O$	$C_{12}H_{25}Me_3NBr$	61		3	5	228	32	76
13	$RuO_2 \cdot xH_2O$	Bu_4PBr	100	PPh_3	30	31	168	185	133
14	$RuO_2 \cdot xH_2O$	Bu_4PBr	100	Ph_3PO	37	45	246	178	201
15	$RuO_2 \cdot xH_2O$	Bu_4PBr	100	TDPME[g]	17	21	138	140	78
16	$RuO_2 \cdot xH_2O$	Bu_4PBr	100[h]		13	9	158	45	87

[a] Charge: Ru, 4.0 mmol; R_4PX, 15 g; run conditions: 220 °C; 430 atm constant pressure; CO/H_2 (1:1), 6–18 h. [b] Analysis of crude liquid product by GLC using modified porous polymer column, programmed from 140–250 °C, at 20 cm³/min He flow; smaller quantities of water, methyl formate, 1-propanol, 1-butanol, and propylene glycol were also detected; carbon dioxide and methane are present in the product gas samples along with much larger quantities of unreacted CO/H_2. [c] Ethylene glycol monoalkyl ether, $HOCH_2CH_2OR$; R = Me, Et, Pr. [d] Liquid yield (wt %) calculated basis total catalyst charge. [e] Total ethylene glycol acetate esters, $HOCH_2CH_2OAc + (CH_2OAc)_2$. [f] Plus significant quantity of methyl acetate. [g] TDPME, 1,1,1-tris[(diphenylphosphino)methyl]ethane; P/Ru mole ratio = 1. [h] Run time, 2 h.
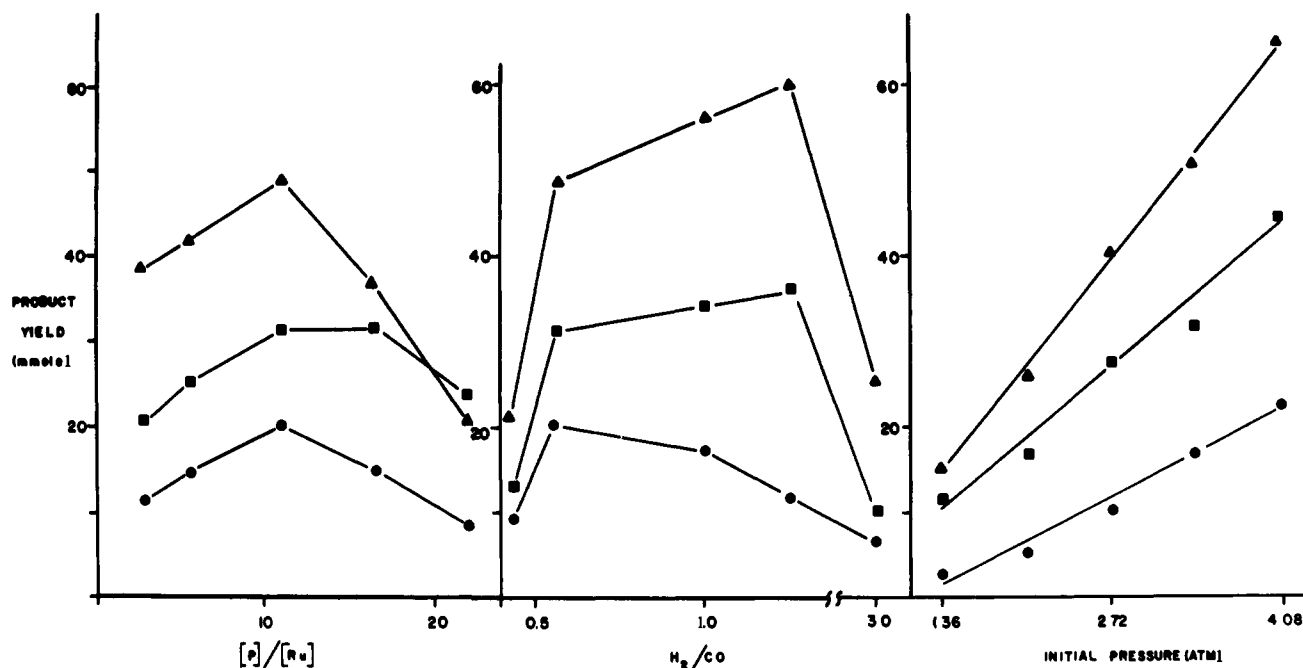

Figure 1. Ethylene glycol from synthesis gas. Total ethylene glycol (glycol plus glycol monoalkyl ether), ●; total methanol, ▲; ethanol, ■. Effect of [P]/[Ru] ratio (typical operating conditions: $RuO_2 \cdot xH_2O$, 2.67 mmol; CO/H_2 = 3:2; 220 °C; 6 h; 340 atm initial pressure), H_2/CO ratio (typical operating conditions: $RuO_2 \cdot xH_2O$, 2.67 mmol; Bu_4PBr, 10 g; 220 °C; 6 h; 340 atm initial pressure), and initial pressure (typical operating conditions: $RuO_2 \cdot xH_2O$; 2.67 mmol; Bu_4PBr, 10 g; CO/H_2 = 3:2; 220 °C; 6 h.

product, and the solid residual ruthenium catalyst recycled.[9] Anhydrous ruthenium(IV) oxide dispersed in tetrabutylphosphonium bromide, for example (Table I, expt 1), typically generates liquid weight gains of 166% of which 34 wt% is ethylene glycol and its monoalkyl ether derivatives.

A variety of quaternary group 5B salts has been considered for these syntheses[9] (see Table I). The primary requirements are that the salts be thermally stable under typical CO hydrogenation conditions and that they melt below the reaction temperature to give a homogeneous, highly polar, fluid medium for solubilization of the ruthenium catalyst precursor. Certain quaternary ammonium salts proved unsatisfactory due to competing Hofmann degradation.[11] Little or no CO hydrogenation was detected in

the presence of quaternary arsonium or stibonium salts. Glycol esters, particularly ethylene glycol monoacetate, are evident with the RuO_2/Bu_4POAc combination (Table I, expt 9). The syntheses are generally believed to be homogeneous, since hydrocarbons higher than methane are rarely detected,[12] there is no evidence of ruthenium metal plating,[13] and the product distribution remains essentially unchanged during multiple catalyst cycling.[9]

The essential features of this catalysis have been probed further through spectroscopic and rate measurements. Following CO hydrogenation (Table I, expt 1–3,6), the typical deep-red liquid products exhibit infrared (ν_{CO} 2060 w, 2018 s, 1991 s, 1956 m cm⁻) and ¹H NMR spectra (−13 ppm) characteristic[14] of the

(11) Jain, S. R.; Rao, M. V.; Verneker, V. R. *Proc. Indian Acad. Sci., Sect. A* **1978**, *87A*, 31.

(12) Bradley, J. S. *J. Am. Chem. Soc.* **1979**, *101*, 7419.

(13) All experiments were conducted in pressure reactors with removable glass liners under the conditions specified in Table I.

anionic triruthenium hydrocarbonyl cluster, $[HRu_3(CO)_{11}]^-$. After recovery of the organic (alcohol + diol) product fractions by distillation in vacuo, the solid residual catalysts display spectral bands characteristic[12] of $Ru(CO)_5$ and tetrabutylphosphonium bromide.[15] Recycle of this solid residue with additional syngas again gives rise to liquid product containing $[HRu_3(CO)_{11}]^-$. However, after multicycling, product solutions oftentimes evidence other ν_{CO} bands more typical of related polynuclear ruthenium hydrocarbonyls.[16–19] including $[H_3Ru_4(CO)_{12}]^-$, $[HRu_4(CO)_{13}]^-$ and $[HRu_6(CO)_{18}]^-$.
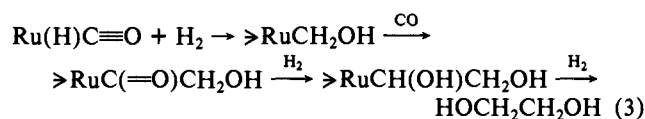
The ruthenium hydrocarbonyl cluster $[HRu_3(CO)_{11}]^-$, when evaluated as a model ruthenium catalyst precursor dispersed in Bu_4PBr (expt 4), exhibited comparable glycol productivity to other ruthenium catalyst precursors. The neutral hydrocarbonyl cluster $H_4Ru_4(CO)_{12}$ also performed well, but the $[Ru_6(CO)_{18}]^{2-}$ cluster proved less effective (expt 5). A series of runs with the RuO_2/Bu_4PBr couple plus various group 5B donor ligands[6] (expt 13–15), including phosphines, phosphites, and chelating (potentially tridentate,[20] tripod) ligands, as well as phosphine oxides favored in related glycol syntheses,[21] provided at best only modest improvements in glycol molar selectivity.

Other investigations into the factors favoring improved glycol productivity (Figure 1) indicate a linear dependence of oxygenate yield upon operating pressure and a sensitivity to feed gas composition. Although the stoichiometry of eq 1 calls for hydrogen-rich synthesis gas, an examination into the effect of CO/H_2 ratios upon glycol yield (Figure 1) suggests that 1:1 or CO-rich gas is preferable. This may be due in part to the need for high CO partial pressures to stabilize polynuclear ruthenium hydrocarbonyls at temperatures >200 °C. Increased hydrogen partial pressures generally favor improved alkanol production (Figure 1), possibly because of more facile hydrogenation capability or the presence of mononuclear ruthenium species that more readily catalyze methanol formation.[12] The situation is further complicated, however, by the fact that during each of these syntheses additional hydrogen is continually being generated in situ via competing, ruthenium-catalyzed, water-gas shift.[9,22]

Ruthenium catalysis, in contrast to homogeneous rhodium-catalyzed glycol synthesis,[1] appears to necessitate large quantities of bulky cation, such as the tetrabutylphosphonium cation, in order to achieve maximum glycol productivity. This appears true both for glycol synthesis via melt catalysis (Figure 1) and for the production of vicinal glycol esters.[6,8] Certainly the preferred Ru:P ratios of Figure 1 are contrary to any known charge ratio for either ruthenium hydrocarbonyl monomeric or cluster species. It likely reflects maximum solubility limits for the ruthenium species in the quaternary salt and/or the need to favor ion pairing.

The subsequent steps of CO hydrogenation to glycol may follow a hydroxymethylene growth reaction path as proposed earlier for rhodium homogeneous catalysis.[1] Our observed product distribution (ethylene glycol, glycol monoalkyl ethers, and ethanol, Table I), including the formation of trace quantities of propylene glycol, would be in keeping with the type of chain-growth scheme

depicted here in eq 3[1,4] for ethylene glycol formation. (Hydroxymethyl)ruthenium intermediates have been proposed in

$$Ru(H)C{\equiv}O + H_2 \rightarrow \text{>}RuCH_2OH \xrightarrow{CO}$$
$$\text{>}RuC({=}O)CH_2OH \xrightarrow{H_2} \text{>}RuCH(OH)CH_2OH \xrightarrow{H_2}$$
$$HOCH_2CH_2OH \quad (3)$$

related oxo catalysis[23] but isolated only for the earlier transition metals.[24] An alternative mechanstic scheme might involve formylruthenium clusters[25] or ruthenium coordinated to formaldehyde,[7] but in melt catalysis we find no enhancement in glycol productivity upon adding formaldehyde.

The extension of this unique fluid melt catalysis to related syntheses remains under study.

(23) Sanchez-Delgado, R. A.; Bradley, J. S.; Wilkinson, G *J. Chem. Soc., Dalton Trans.* **1976**, 399.

(24) Casey, C. P.; Andrews, M. A.; McAlister, D. R. *J. Am. Chem. Soc.* **1979**, *101*, 3378.

(25) Pruett, R. L.; Schoening, R. C.; Vidal, J. L.; Fiato, R. A. *J. Organomet. Chem.* **1979**, *182*, C57.

Ligand-Induced Valence Tautomerism in Manganese–Quinone Complexes

Michael W. Lynch and David N. Hendrickson*

School of Chemical Sciences, University of Illinois Urbana, Illinois 61801

Brian J. Fitzgerald and Cortlandt G. Pierpont*

Department of Chemistry, University of Colorado Boulder, Colorado 80309

Recent studies have linked oxygen production by photosynthetic bacteria with a manganese-containing cofactor associated with photosystem II in plant chloroplasts.[1–6] Analytical results carried out to determine the number of chloroplast bound manganese atoms compared with data on the relative flash yield of O_2 suggest 3–4 functional Mn atoms per cofactor.[3,7] Other experiments seem to indicate the presence of Mn(II) and Mn(III) ions.[8,9] This has been confirmed by recent XAEFS/EXAFS experiments which further suggest that each Mn has a second transition-metal nearest neighbor, possibly a second Mn atom.[9,10] It is also known that 1,4-benzoquinones are included in the photosynthetic electron-transport chain,[11] although there is no direct evidence linking them to the Mn centers. Sawyer and co-workers have made some pertinent observations on the ability of manganese–catecholate complexes to reversibly bind molecular oxygen.[12,13] Reduction

(14) Johnson, B. F. G.; Lewis, J.; Raithby, P. R.; Suss, G. *J. Chem. Soc., Dalton Trans.* **1979**, 1356.

(15) Residual solid ruthenium melt catalyst samples were also routinely subject to elemental analyses (5 elements), IR spectroscopy and m.p. determination (82–88 °). Data were consistent with the tetrabutylphosphonium bromide formulation. Dealkylation of the phosphonium salt did not appear to be a problem. Ruthenium analysis of these same solid catalyst samples showed no significant selective loss of ruthenium.

(16) Inkrott, K. E.; Shore, S. G. *Inorg. Chem.* **1979**, *18*, 2817.

(17) Eady, C. R.; Jackson, P. F.; Johnson, B. F. G.; Lewis, J.; Malatesta, M. C.; McPartlin, M.; Nelson, W. J. H. *J. Chem. Soc., Dalton Trans.* **1980**, 383.

(18) Koepke, J. W.; Johnson, J. R.; Knox, S. A. R.; Kaesz, H. D. *J. Am. Chem. Soc.* **1975**, *97*, 3947.

(19) Nagel, C. C.; Shore, S. G. *J. Chem. Soc., Chem. Commun.* **1980**, 530.

(20) DeBoer, J. J.; Van Doom, J. A.; Masters, C. *J. Chem. Soc., Chem. Commun.* **1978**, 1005.

(21) Kaplan, L. European Patent 0 006 634, 1980.

(22) Ford, P. C.; Rinker, R. G.; Ungermann, C.; Laine, R. M.; Landis, V.; Moya, S. A. *J. Am. Chem. Soc.* **1978**, *100*, 4595. Ford, P. C.; Ungermann, C.; Landis, V.; Moya, S. A.; Rinker, R. G.; Laine, R. M. *Adv. Chem. Ser.* **1979**. *No. 173*, 81.

(1) Joliot, P.; Kok, B. In "Bioenergetics of Photosynthesis"; Govindjee, Ed.; Academic Press: New York, 1975.

(2) Mar, T.; Govindjee *J. Theor. Biol.* **1972**, *36*, 427–446.

(3) Cheniae, G. *Annu. Rev. Plant Physiol.* **1970**, *21*, 467–498.

(4) Earley, J. E. *Inorg. Nucl. Chem. Lett.* **1973**, *9*, 487–490.

(5) Renger, G., *Z. Naturforsch., Sect. B* **1970**, *B25*, 966–971.

(6) Olson, J. M. *Science* (Washington, DC) **1970**, *168*, 438.

(7) Govindjee; Wydrzynski, T.; Marks, S. B. In "Bioenergetics of Membranes"; Pacher, L., Papageorgious, G. C., Trebst, A., Eds.; Elsevier: Amsterdam, 1977.

(8) Rener, G. In "Photosynthetic Water Oxidation"; Metzer, H., Ed.; Academic Press: London, 1978.

(9) Sauer, K. *Acc. Chem. Res.* **1980**, *13*, 249–256.

(10) Kirby, J.; Robertson, A. S.; Smith, J. P.; Thompson, A. C.; Goodin, D. B.; Klein, M. unpublished work, quoted in ref 9.

(11) Crofts, A. R. In "Light-Induced Charge Separation in Biology and Chemistry"; Gerischer, H., Katz, J. J., Eds.; Dahlem Konferenzen: Berlin, 1979.